J Eng Math (2009) 65:157–169
DOI 10.1007/s10665-009-9271-5

Power-series solution for the two-dimensional inviscid flow with a vortex and multiple cylinders

Oktay K. Pashaev · Oguz Yilmaz

Received: 9 June 2008 / Accepted: 27 January 2009 / Published online: 17 February 2009

Abstract The problem of a point vortex and N fixed cylinders in a two-dimensional inviscid fluid is studied and an analytical-numerical solution in the form of an infinite power series for the velocity field is obtained using complex analysis. The velocity distribution for the case of two cylinders is compared with the existing results of the problem of a vortex in an annular region which is conformally mapped onto the exterior of two cylinders. Limiting cases of N cylinders and the vortex, being far away from each other are studied. In these cases, "the dipole approximation" or "the point-island approximation" is derived, and its region of validity is established by numerical tests. The velocity distribution for a geometry of four cylinders placed at the vertices of a square and a vortex is presented. The problem of vortex motion with N cylinders addressed in the paper attracted attention recently owing to its importance in many applications. However, existing solutions using Abelian function theory are sophisticated and the theory is not one of the standard techniques used by applied mathematicians and engineers. Moreover, in the $N \geq 3$ cylinder problem, the infinite product involved in the presentation of the Schottky–Klein prime function must also be truncated. So, the approach used in the paper is simple and an alternative to existing methods. This is the main motivation for this study.

Keywords Circle theorem · Hydrodynamic interaction · Point vortex · Power-series solution · Vortex dynamics

1 Introduction

Hydrodynamic interaction among surface-piercing cylinders and water waves has been studied by many authors such as Spring and Monkmeyer [1], Kagemoto and Yue [2], Linton and Evans [3] and Yilmaz [4]. An extensive review of the literature is given by Martin [5, Chap. 4]. Common to all of these studies is the partial wave decomposition of incoming and diffracted waves in terms of Bessel functions and the unknown coefficients introduced at each partial wave component. After the decomposition, the boundary conditions imposed at the boundary of each cylinder lead to an infinite system of linear equations to determine the unknown coefficients. However, in all of

O. K. Pashaev · O. Yilmaz (✉)
Department of Mathematics, Izmir Institute of Technology, Urla, Izmir 35430, Turkey
e-mail: oguzyilmaz@iyte.edu.tr

O. K. Pashaev
e-mail: oktaypashaev@iyte.edu.tr

these studies the fluid flow has been assumed to be irrotational. Extension of these results to the case of rotational flow requires an understanding of the fluid flow around cylinders in the presence of vortices.

The goal of the present paper is to study one vortex problem in the presence of N cylinders by decomposing the velocity field of a vortex in an infinite power series. Interaction that takes place is resolved in a similar fashion to the problem of diffracted surface waves. Namely, the flow of a vortex without cylinders replaces the incident waves and the effect of cylinders is treated as diffracted waves.

The problem of a vortex with two cylinders can be conformally mapped onto the vortex problem in an annular domain. It admits an exact analytic solution in terms of elliptic functions and has been studied by Johnson and McDonald [6], Burton et al. [7] and Crowdy and Marshall [8]. Analysis of the same problem by the method of images in terms of the q-calculus has been examined by the present authors in [9]. In the present paper, the previous study is extended to the problem of a vortex with an arbitrary number of cylinders in a two-dimensional unbounded fluid domain. It is assumed that fluid motion is irrotational and a line vortex is introduced into the fluid domain. The vortex problem in multiply connected domains has been studied by Crowdy and Marshall [8], [10] and [11] from the point of view of Möbius maps and the Schottky–Klein group. The Schottky–Klein prime function for the annulus is related to the first Jacobi theta function and the methods mentioned above, which uses the elliptic function and the q-logarithmic function, give the same result. The q-calculus construction of the Schottky–Klein prime function [9] suggests that this function is a composed object of more elementary q-exponential functions, also appearing as the quantum dilogarithm, and could be important in the theory of automorphic functions and for multiply connected domains. Unfortunately, in the multi-cylinder case the explicit form of this function is unknown. This is why it is desirable to develop another independent approach to this problem. The method presented in this paper is an alternative mathematical construction of the problem by complex analysis. The mathematical solution of the problem was obtained by the authors mentioned above using Abelian function theory. This method is quite sophisticated and abstract and is not part of the standard mathematical syllabus. Due to wide applications of the problem it is desirable to obtain a solution of the problem by some standard techniques, affordable by applied mathematicians and engineers. This is the main motivation for our work.

In this paper a series-based method is used which directly sums the image effects of the vortex in each of the cylinders and the images of these images and so on. Coefficients of this series are found by numerical solution of a truncated linear system and is thus approximate in this sense. It may be worth noting that in the $N \geq 3$ cylinder problem the infinite product involved in the representation of the Schottky–Klein prime function [8,10,11] must also be truncated. In [8] it is mentioned that the convergence properties of the infinite products defining the Schottky–Klein prime function is a complicated mathematical issue and that the products are truncated at suitable levels to ensure convergence.

The power-series method is not new. Indeed, introducing source, doublet or vortex distributions of unknown strength and then applying the boundary conditions to determine the coefficients was carried out by Katz and Plotkin [12, Chap. 6]. Also, Fourier–Bessel series are used in hydrodynamic interaction theory by Linton and Evans [3]. We are claiming that solution of the present problem by this technique is new, simple and alternative to the existing solutions by Crowdy and Marshall [8] and Johnson and McDonald [13]. The series-expansion method for solving both the biharmonic and harmonic equations are studied in [14] where the velocity field for two-dimensional flow in a batch stirring device is determined following the work of Price et al. [15]. Hellou and Coutanceau [16] devised a hybrid polar/Cartesian system to investigate the cellular flow induced by a rotating cylinder in a rectangular channel. In all of the last three articles the domain is bounded. However, in contrast to the above paper which treats the boundary condition by truncating the series expansion and then choosing coefficients to a best fit for the velocity field at the boundary, in our approach we satisfy the boundary condition exactly.

The paper is organized as follows. In Sect. 2 we formulate the problem of a vortex and N cylinders by the Laurent series expansion with unknown coefficients. In order to determine these coefficients we apply the boundary conditions and arrive at an infinite linear algebraic system of equations determined by the geometry of the cylinders and position of the vortex. In Sect. 3 for any potential user, not interested in mathematical detail, we explain a step-by-step algorithmic procedure to calculate the velocity field at any point of the domain. For solving the linear algebraic system in Sect. 4 we apply numerical methods. To verify our results, first we solve the two-cylinder

problem and compare the results with the solution of the annular-domain problem which can be mapped onto the former problem by a conformal mapping. Then, for an arbitrary number of cylinders far from each other and the vortex, we derive the dipole (the point-island) approximation. In this case we consider the vortex motion around N cylinders, illustrating numerical calculations by figures. Finally in the Conclusions we discuss the main results and the similarities/differences with other papers.

2 Formulation of the problem

We formulate the problem of one vortex and N stationary cylinders in an unbounded two-dimensional domain in several steps starting with the well-known case of a single vortex and a single cylinder. For simplicity we shall take all the circulations around the cylinders to be zero. The more general case can be easily obtained by including in (9), (10) simple pole terms with $n = 0$. In what follows z denotes the complex variable $x + \mathrm{i}y$.

2.1 A vortex and a cylinder

First, consider a vortex of strength κ at z_0 and a cylinder of radius a at the origin. The complex velocity potential is given by the Circle Theorem of Milne-Thomson [17, Sect. 6.21],

$$\omega = \mathrm{i}\kappa \log(z - z_0) - \mathrm{i}\kappa \log\left(\frac{a^2}{z} - \bar{z}_0\right), \tag{1}$$

$$= \mathrm{i}\kappa \log(z - z_0) - \mathrm{i}\kappa \log\left(z - z_0'\right) + \mathrm{i}\kappa \log(z) - \mathrm{i}\kappa \log(-\bar{z}_0), \tag{2}$$

where $\bar{z}_0 = a^2/z_0'$ and z_0' is called the inverse point of z_0 with respect to the cylinder. Equation 2 implies that the effect of the cylinder introduced at the origin is two extra vortices; one of these is at the inverse point of z_0 with negative strength and another at the centre of the cylinder with positive strength. Henceforth, we shall call the vortices at inverse points and at the centres of cylinders (or at infinity) "vortex images" or simply "images". Therefore, the previous statement can be rephrased as "the effect of the cylinder, introduced at the origin, to the potential is two images, one at the inverse point with negative strength and the other at the centre with positive strength".

In order to simplify the calculations and avoid dealing with multi-valuedness of the logarithmic function, it will be advantageous to work with the complex velocity rather than complex potential,

$$\bar{V} = \frac{\mathrm{i}\kappa}{z - z_0} - \frac{\mathrm{i}\kappa}{z - z_0'} + \frac{\mathrm{i}\kappa}{z}, \tag{3}$$

where $\bar{V} = \dfrac{\mathrm{d}\omega}{\mathrm{d}z} = u - \mathrm{i}v$. Next, we consider a vortex of strength κ at z_0 and a cylinder of radius a_j at z_j. In this case, the complex velocity is obtained by translating the coordinates to z_j in (3),

$$\bar{V} = \frac{\mathrm{i}\kappa}{z - z_0} - \frac{\mathrm{i}\kappa}{z - z_j - \left(z_0 - z_j\right)'} + \frac{\mathrm{i}\kappa}{z - z_j}$$

$$= \frac{\mathrm{i}\kappa}{\zeta_j - \zeta_{0j}} - \frac{\mathrm{i}\kappa}{\zeta_j - \zeta_{0j}'} + \frac{\mathrm{i}\kappa}{\zeta_j} = \bar{V}_j^I + \bar{V}_j^D, \tag{4}$$

where $\zeta_j = z - z_j$ and $\zeta_{0j} = z_0 - z_j$. It should be noted that (4) satisfies the Circle Theorem. The term $\bar{V}_j^I = \frac{\mathrm{i}\kappa}{\zeta_j - \zeta_{0j}}$ in (4) represents the velocity field due to the vortex alone and the superscript I stands for "incident waves" by making the analogy with the problem of "hydrodynamic interaction between water waves and cylinders" which the second author investigated previously [4]. Similarly, the term $\bar{V}_j^D = -\frac{\mathrm{i}\kappa}{\zeta_j - \zeta_{0j}'} + \frac{\mathrm{i}\kappa}{\zeta_j}$ represents the effect of the cylinder on the velocity field and the superscript D stands for "diffracted waves" again by analogy with the water-wave diffraction problem.

Now, the terms in (4) are expanded into a Laurent series around z_j. We start with,

$$\bar{V}_j^I = \frac{\mathrm{i}\kappa}{\zeta_j - \zeta_{0j}} = -\frac{\mathrm{i}\kappa}{\zeta_{0j}} \sum_{n=0}^{\infty} \left(\frac{\zeta_j}{\zeta_{0j}}\right)^n, \quad |\,\zeta_j\,| < |\,\zeta_{0j}\,|. \tag{5}$$

Here we assume that the centre of the vortex is outside the cylinder. In this case the condition, $|\,\zeta_j\,| < |\,\zeta_{0j}\,|$, is certainly true when the boundary condition is applied on the cylinder, $z = z_j + a_j \mathrm{e}^{\mathrm{i}\theta_j}$.

The last two terms in (4) are treated together,

$$\bar{V}_j^D = \frac{\mathrm{i}\kappa}{\zeta_j} - \frac{\mathrm{i}\kappa}{\zeta_j - \zeta'_{0j}} = -\mathrm{i}\kappa \sum_{n=1}^{\infty} \frac{\left(\zeta'_{0j}\right)^n}{\zeta_j^{n+1}}, \tag{6}$$

where $\zeta'_{0j} = \frac{a_j^2}{\bar{\zeta}_{0j}}$ implies $|\zeta'_{0j}| \le |\zeta_j|$, and corresponds to the vortex images.

2.2 A vortex and N cylinders

Now we assume that there are N cylinders of radii $a_1, \ldots, a_N$ placed in an unbounded two-dimensional fluid domain at points $z_1, \ldots, z_N$ and that a vortex is placed at z_0 outside the cylinders. In order to apply the boundary condition at the boundaries of the cylinders, we express the total velocity near cylinder j as,

$$\bar{V}_j^T = \bar{V}_j^I + \bar{V}_j^D + \sum_{i=1(i\neq j)}^{N} \bar{V}_i^D, \tag{7}$$

where

$$\bar{V}_j^I = -\frac{\mathrm{i}\kappa}{\zeta_{0j}} \sum_{n=0}^{\infty} \left(\frac{\zeta_j}{\zeta_{0j}}\right)^n, \quad |\,\zeta_j\,| < |\,\zeta_{0j}\,|, \tag{8}$$

$$\bar{V}_j^D = -\mathrm{i}\kappa \sum_{n=1}^{\infty} A_n^j \frac{\left(\zeta'_{0j}\right)^n}{\zeta_j^{n+1}}, \quad |\,\zeta'_{0j}\,| < |\,\zeta_j\,|, \tag{9}$$

$$\bar{V}_i^D = -\mathrm{i}\kappa \sum_{n=1}^{\infty} A_n^i \frac{\left(\zeta'_{0i}\right)^n}{\zeta_i^{n+1}} = -\mathrm{i}\kappa \sum_{n=1}^{\infty} A_n^i \frac{\left(\zeta'_{0i}\right)^n}{\left(\zeta_j + R_{ij}\right)^{n+1}} \tag{10}$$

and A_n^i are unknown complex coefficients. Notice that in (10) the coordinate transformation is carried out using the relation $\zeta_i = \zeta_j + R_{ij}$, where $R_{ij} = z_j - z_i$. Notice that the condition in (9), $|\,\zeta'_{0j}\,| < |\,\zeta_j\,|$, is always satisfied unless the vortex is inside the cylinder and that the condition, $|\zeta_j\,| < |\,\zeta_{0j}|$, is certainly satisfied on the boundary of cylinder j where the boundary condition is applied. Also, we see that for the case of a single cylinder the unknown coefficient A_n^j in (9) becomes unity. Here the first term in (7) represents the velocity field due to the vortex, whereas the second and third terms account for the effects of the cylinders and they describe a set of images in cylinders and the images of images. As we already mentioned in the Introduction, the idea is borrowed from the hydrodynamic interaction of surface waves with vertical circular cylinders, where the diffracted waves are expanded into a power series with unknown complex coefficients using the decomposition of incident waves. By analogy, here the flow of a vortex alone replaces the incident waves and the effect of the cylinders is treated as diffracted waves. As we mentioned above, the more general case with nonvanishing circulation around the cylinders can be easily treated by inclusion in the summations (9), (10) a simple pole-term contribution with $n = 0$.

The boundary condition to be satisfied for each cylinder is that "the normal component of $\overline{V}_j^T = 0$, when $|\zeta_j| = a_j, \forall j$". This condition is equivalent to the statement

$$a_j \mathfrak{Re}\left(\bar{V}_j^T \mathrm{e}^{\mathrm{i}\theta_j}\right) = \mathfrak{Re}\left(\bar{V}_j^T a_j \mathrm{e}^{\mathrm{i}\theta_j}\right) = \mathfrak{Re}\left(\bar{V}_j^T \zeta_j\right) = 0, \quad j = 1, \ldots, N, \tag{11}$$

where $\mathfrak{Re}(z)$ denotes the real part of z. In the last equality $\zeta_j = a_j e^{i\theta_j}$ is used, this holds only on the boundary of cylinder j. Application of this condition yields

$$\mathfrak{Re}\left[-i\kappa\left[\sum_{n=0}^{\infty}\frac{\zeta_j^{n+1}}{\zeta_{oj}^{n+1}}+\sum_{n=1}^{\infty}\frac{B_n^j}{\zeta_j^n}+\sum_{i=1}^{N}(1-\delta_{ij})\sum_{n=1}^{\infty}\frac{B_n^i\zeta_j}{(\zeta_j+R_{ij})^{n+1}}\right]\right]_{|\zeta_j|=a_j}=0, \tag{12}$$

where $B_n^j = A_n^j \frac{a_j^{2n}}{\bar{\zeta}_{0j}^n}$ and $\delta_{ij} = 1$ when $i = j, \delta_{ij} = 0$ otherwise. The last term in (12) must be expanded into a series to make the calculations simpler, viz.

$$\frac{1}{(\zeta_j+R_{ij})^{n+1}}=\frac{1}{R_{ij}^{n+1}}\sum_{k=0}^{\infty}\frac{(n+1)_k}{k!}\left(-\frac{\zeta_j}{R_{ij}}\right)^k, \tag{13}$$

where $(n+1)_k = (n+1)(n+2)\ldots(n+k)$ is the Pochhammer symbol and $(n+1)_0 = 1$. Equation 12 is equivalent to,

$$i\left[\sum_{n=0}^{\infty}\frac{\zeta_j^{n+1}}{\zeta_{oj}^{n+1}}+\sum_{n=1}^{\infty}\frac{B_n^j}{\zeta_j^n}+\sum_{i=1}^{N}(1-\delta_{ij})\sum_{n=1}^{\infty}\frac{B_n^i\zeta_j}{R_{ij}^{n+1}}\sum_{k=0}^{\infty}\frac{(n+1)_k}{k!}\left(\frac{-\zeta_j}{R_{ij}}\right)^k\right]+c.c.=0 \tag{14}$$

when $|\zeta_j| = a_j$, where $c.c.$ stands for the complex conjugation. Using $\zeta_j\bar{\zeta}_j = a_j^2$ in (14) leads to

$$\sum_{n=0}^{\infty}\left(\frac{\zeta_j}{\zeta_{0j}}\right)^{n+1}+\sum_{i=1}^{N}(1-\delta_{ij})\sum_{n=1}^{\infty}\frac{B_n^i}{R_{ij}^{n+1}}\sum_{k=0}^{\infty}(-1)^k\frac{(n+1)_k}{k!}\frac{\zeta_j^{k+1}}{R_{ij}^k}-\sum_{n=1}^{\infty}\frac{\zeta_j^n\overline{B}_n^j}{a_j^{2n}}=0. \tag{15}$$

This transition has a simple explanation. Equation 14 has the form of a Laurent series:

$$\sum_{n=0}^{\infty}\alpha_n\zeta^n+\sum_{n=1}^{\infty}\frac{\beta_n}{\zeta^n}+\sum_{n=0}^{\infty}\bar{\alpha}_n\bar{\zeta}^n+\sum_{n=1}^{\infty}\frac{\bar{\beta}_n}{\bar{\zeta}^n}=0. \tag{16}$$

By the circle condition $\zeta\bar{\zeta} = a^2$ it can be represented as

$$\left(\sum_{n=0}^{\infty}\alpha_n\zeta^n+\sum_{n=1}^{\infty}\frac{\bar{\beta}_n}{a^{2n}}\zeta^n\right)+\left(\sum_{n=0}^{\infty}\bar{\alpha}_n\bar{\zeta}^n+\sum_{n=1}^{\infty}\frac{\beta_n}{a^{2n}}\bar{\zeta}^n\right)=0 \tag{17}$$

or

$$\sum_{n=0}^{\infty}\left(\alpha_n+\frac{\bar{\beta}_n}{a^{2n}}\right)\zeta^n+\sum_{n=0}^{\infty}\left(\bar{\alpha}_n+\frac{\beta_n}{a^{2n}}\right)\bar{\zeta}^n=0, \tag{18}$$

where $\beta_0 = 0$. Due to $\zeta = ae^{i\theta}$, and the orthogonality of $\zeta^n = a^n e^{in\theta}$ and $\zeta^m = a^m e^{im\theta}$ for integer values n and m, when $n \neq m$, the first sum is orthogonal to the second one, and every term in the first sum is orthogonal to the other terms in the same sum. This is why in (15) we take only one sum without its complex conjugate. Equating every coefficient for given n to zero gives an algebraic system for the unknown coefficients B_l^s,

$$\sum_{l=1}^{\infty}\sum_{s=1}^{N}D_{nl}^{js}B_l^s=C_n^j,\quad j=1,\ldots,N,\quad n=0,1,\ldots, \tag{19}$$

where

$$D_{nl}^{js}=-\frac{\delta_{n+1,l}^{j,s}}{a_j^{2n+2}}+\frac{(-1)^n}{n!}\sum_{k=1}^{\infty}\sum_{i=1}^{N}(1-\delta_{si})(1-\delta_{ij})\frac{(-1)^{k-1}}{(k-1)!}\frac{a_i^{2k}(k+1)_n(l+1)_{k-1}}{R_{si}^{k+l}\overline{R}_{ij}^{n+k+1}}, \tag{20}$$

$$C_n^j=\frac{-1}{\bar{\zeta}_{0j}^{n+1}}-\frac{(-1)^n}{n!}\sum_{i=1}^{N}(1-\delta_{ij})\sum_{k=1}^{\infty}\frac{(k+1)_n a_i^{2k}}{\overline{R}_{ij}^{n+k+1}}\frac{1}{\zeta_{0i}^k}, \tag{21}$$

where $\delta^{j,s}_{n+1,l} = \delta_{n+1,l}\delta_{j,s}$. Notice that with a single cylinder, the above system gives $B_n = a_j^{2n}/\bar{\zeta}^n_{0j}$, which is equivalent to $A_n = 1$ as expected.

Since there is no vortex inside the cylinders, the force on them should be zero by the Kutta–Joukowski Theorem. The Blasius' Theorem is employed to verify this assumption. The square of the velocity is needed for this purpose, that is,

$$\left(V_j^T\right)^2 = \left(V_j^I + V_j^D + \sum_{i=1(i\neq j)}^{N} V_i^D\right)^2 = \left(V_j^I\right)^2 + 2V_j^I \sum_{i=1}^{N} V_i^D + \sum_{i=1}^{N}\sum_{k=1}^{N} V_i^D V_k^D, \tag{22}$$

where

$$\left(\bar{V}_j^I\right)^2 = \frac{-\kappa^2}{\zeta_{0j}^2}\sum_{n=0}^{\infty}\sum_{m=0}^{\infty}\left(\frac{\zeta_j}{\zeta_{0j}}\right)^{n+m},$$

$$\bar{V}_j^I\bar{V}_i^D = \frac{-\kappa^2}{\zeta_{0j}}\sum_{n=0}^{\infty}\sum_{m=1}^{\infty}\sum_{k=0}^{\infty} A_m^i\zeta_j^{n+k}\frac{\left(\zeta_{0i}'\right)^m}{\left(\zeta_{0j}\right)^n}\frac{(-1)^k(m+1)_k}{k!R_{ij}^{k+m+1}},$$

$$\bar{V}_i^D\bar{V}_k^D = -\kappa^2\sum_{n=1}^{\infty}\sum_{m=1}^{\infty}\sum_{k=0}^{\infty}\sum_{l=0}^{\infty} A_m^i A_n^i\zeta_j^{k+l}\frac{\left(\zeta_{0i}'\right)^{m+n}}{R_{ij}^{k+l+m+n+2}}\frac{(-1)^{k+l}(m+1)_l(n+1)_k}{k!l!}.$$

If we integrate (22) with respect to ζ_j around cylinder j, we see that all terms give a zero contribution,

$$\Im\mathfrak{m} = \frac{-\mathrm{i}\rho}{2}\overline{\left[\int\left(\bar{V}_j^T\right)^2 \mathrm{d}\zeta_j\right]} = 0, \tag{23}$$

where ρ denotes the mass density of the fluid.

3 An algorithm for calculating the velocity field

1. Input the positions of the centres of the cylinders, (x_j, y_j), the radius of each cylinder, a_j, $j = 1, \ldots, N$, and the initial position of the vortex, (x_0, y_0);
2. Take a truncation level, say, $S = 20$;
3. There are $N * S$ unknowns, B_l^s, $l = 1, \ldots, S$, $s = 1, \ldots, N$, to be determined. Form the matrices D and C

$$D = \left[\begin{array}{cccc|cccc|c|c}
D_{01}^{11} & D_{01}^{12} & \cdots & D_{01}^{1S} & D_{02}^{11} & D_{02}^{12} & \cdots & D_{02}^{1S} & \cdots & D_{0S}^{1S} \\
D_{11}^{11} & D_{11}^{12} & \cdots & D_{11}^{1S} & D_{12}^{11} & D_{12}^{12} & \cdots & D_{12}^{1S} & \cdots & D_{1S}^{1S} \\
\vdots & \vdots & \vdots & \vdots & \vdots & \vdots & \vdots & \vdots & \cdots & \vdots \\
D_{(S-1)1}^{11} & D_{(S-1)1}^{12} & \cdots & D_{(S-1)1}^{1S} & D_{(S-1)2}^{11} & D_{(S-1)2}^{12} & \cdots & D_{(S-1)2}^{1S} & \cdots & D_{(S-1)S}^{1S} \\
\hline
D_{01}^{21} & D_{01}^{22} & \cdots & D_{01}^{2S} & D_{02}^{21} & D_{02}^{22} & \cdots & D_{02}^{2S} & \cdots & D_{0S}^{2S} \\
D_{11}^{21} & D_{11}^{22} & \cdots & D_{11}^{2S} & D_{12}^{21} & D_{12}^{22} & \cdots & D_{12}^{2S} & \cdots & D_{1S}^{2S} \\
\vdots & \vdots & \vdots & \vdots & \vdots & \vdots & \vdots & \vdots & \cdots & \vdots \\
D_{(S-1)1}^{21} & D_{(S-1)1}^{22} & \cdots & D_{(S-1)1}^{2S} & D_{(S-1)2}^{21} & D_{(S-1)2}^{22} & \cdots & D_{(S-1)2}^{2S} & \cdots & D_{(S-1)S}^{2S} \\
\hline
\vdots & \vdots & \vdots & \vdots & \vdots & \vdots & \vdots & \vdots & \cdots & \vdots \\
\hline
D_{01}^{N1} & D_{01}^{N2} & \cdots & D_{01}^{NS} & D_{02}^{N1} & D_{02}^{N2} & \cdots & D_{02}^{NS} & \cdots & D_{0S}^{NS} \\
D_{11}^{N1} & D_{11}^{N2} & \cdots & D_{11}^{NS} & D_{12}^{N1} & D_{12}^{N2} & \cdots & D_{12}^{NS} & \cdots & D_{1S}^{NS} \\
\vdots & \vdots & \vdots & \vdots & \vdots & \vdots & \vdots & \vdots & \cdots & \vdots \\
D_{(S-1)1}^{N1} & D_{(S-1)1}^{N2} & \cdots & D_{(S-1)1}^{NS} & D_{(S-1)2}^{N1} & D_{(S-1)2}^{N2} & \cdots & D_{(S-1)2}^{NS} & \cdots & D_{(S-1)S}^{NS}
\end{array}\right]$$

$$C^T = \left[\, C_0^1\ C_1^1\ \cdots\ C_{S-1}^1 \middle| C_0^2\ C_1^2\ \cdots\ C_{S-1}^2 \middle| \cdots \middle| C_0^N\ C_1^N\ \cdots\ C_{S-1}^N \,\right]$$

where

$$D_{nl}^{js} = -\frac{\delta_{n+1,l}^{j,s}}{a_j^{2n+2}} + \frac{(-1)^n}{n!}\sum_{k=1}^{s}\sum_{i=1}^{N}(1-\delta_{si})\left(1-\delta_{ij}\right)\frac{(-1)^{k-1}}{(k-1)!}\frac{a_i^{2k}(k+1)_n(l+1)_{k-1}}{R_{si}^{k+l}\overline{R}_{ij}^{n+k+1}},$$

$$C_n^j = \frac{-1}{\zeta_{0j}^{n+1}} - \frac{(-1)^n}{n!}\sum_{i=1}^{N}\left(1-\delta_{ij}\right)\sum_{k=1}^{s}\frac{(k+1)_n a_i^{2k}}{\overline{R}_{ij}^{n+k+1}}\frac{1}{\zeta_{0i}^{k}};$$

4. Solve the matrix equation $DB = C$ where

$$B^T = \left[\, B_1^1 \;\; B_1^2 \;\cdots\; B_1^N \,\middle|\, B_2^1 \;\; B_2^2 \;\cdots\; B_2^N \,\middle|\cdots\right];$$

5. Determine which of the cylinders' centres, $\left(x_j, y_j\right)$, is closest to the observation point, z;
6. Calculate the velocity at the observation point, z, using the coordinate system of the cylinder determined at the previous step,

$$\bar{V}_j^T = \bar{V}_j^I + \bar{V}_j^D + \sum_{i=1(i\neq j)}^{N}\bar{V}_i^D,$$

where

$$\bar{V}_j^I = -\frac{\mathrm{i}\kappa}{z-z_0},$$

$$\bar{V}_j^D = -\mathrm{i}\kappa\sum_{n=1}^{\infty}A_n^j\frac{\left(\zeta_{0j}'\right)^n}{\zeta_j^{n+1}},$$

$$\bar{V}_i^D = -\mathrm{i}\kappa\sum_{n=1}^{\infty}A_n^i\frac{\left(\zeta_{0i}'\right)^n}{\zeta_i^{n+1}};$$

7. Increase the truncation level to $S+1$, repeat the steps 3 to 6. Calculate the relative error of the velocity obtained by using truncation levels S and $S+1$. If the convergence is sufficient, then stop, if not, continue increasing the truncation level until the desired accuracy is achieved.

4 Numerical results and limiting cases

In order to obtain numerical values, first the infinite system (19) is truncated and then the standard LU decomposition is employed to determine the coefficients. The convergence characteristics of the infinite system is, generally speaking, quite good and is studied in the following subsections. However, when the number of cylinders is large and/or when one of the cylinders' radii is large compared to the others, there is a problem of convergence. This problem is tackled in a recent paper by Antoine et al. [18], where they suggest a fast preconditioned numerical method. They conclude that, in general, the convergence is faster for the preconditioned algorithm.

We carry out the calculations using the coordinate system of a cylinder which is closest to the observation point. The superscript j in coefficient A_n^j represents the cylinder number. So, power series are valid locally and we divide the fluid domain into regions, each of which has one cylinder at the centre. Therefore our "local" approach can be applied to any arbitrary, complicated geometry.

4.1 Two-cylinder problem

The first configuration consists of a vortex placed at (0, 1.618) and two disks of unit radii; one placed at the origin, another at (3, 0) ("Configuration 1") (see Fig. 1). This configuration allows us to compare the results of this study

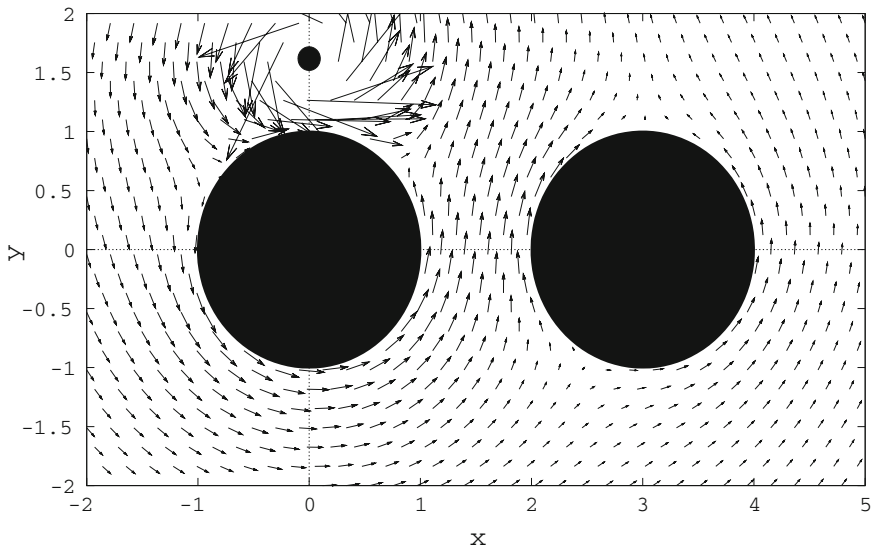

Fig. 1 Velocity distribution around two cylinders with a vortex at (0, 1.618) with strength −0.418. Velocity vectors are scaled down by the factor 1.3

with those of [9] where the same problem has been tackled in an annular region. The configuration considered here can be conformally mapped onto the annular region by

$$\omega = \frac{z-a}{az-1},$$

where $a = \frac{1+c^2-\rho^2+\sqrt{\left((c+\rho^2)^2-1\right)\left((c-\rho^2)^2-1\right)}}{2c}$, ρ is the radius of the circle placed at c on the positive part of the x-axis. The numerical comparison of the convergence of two results shown in Tables 1 and 2 indicates that the "direct solution", which is the one proposed in this paper, converges more slowly than the "indirect solution" of Pashaev and Yilmaz [9]. In order to get 10^{-9} accuracy, the direct solution needs 50 terms, whereas the indirect solution requires only 10 terms. This is expected since the indirect solution is especially designed for the annular region whereas the direct solution can handle an arbitrary number of cylinders in two-dimensional space. Based on Table 1, twenty terms were taken to calculate the velocity field in Fig. 1.

4.2 The point-island approximation

Next, we consider the case when the cylinders are far apart and the point vortex is far away; $\varepsilon_R = \max_{\forall i,j} \frac{a_j}{|R_{ij}|} < \frac{1}{2}$ and $\varepsilon_v = \max_{\forall j} \frac{a_j}{|\zeta_{0j}|} < 1$ are small values. At leading order we get the following,

$$a_j^2 D_{0l}^{js} \approx -\delta_{1,l}^{j,s} + O\left(\varepsilon_R^3\right),$$
$$a_j^2 C_0^j \approx -a_j \varepsilon_v \exp\left(-\mathrm{i}\beta_j\right) + O\left(\varepsilon_R^2\right).$$

If ε_R and ε_v are of the same order or if ε_R is much smaller than ε_v, then B_1^j is by far the most important coefficient,

$$B_1^j = a_j \varepsilon_v \exp\left(-\mathrm{i}\beta_j\right),$$

where $-\beta_j$ is the argument of the complex number ζ_{0j}. Thus, the total velocity near cylinder j is,

$$\bar{V}_j^T = \frac{\mathrm{i}\kappa}{z-z_0} - \mathrm{i}\kappa\varepsilon_v \sum_{i=1}^{N} \frac{a_i}{\zeta_i^2} \exp\left(-\mathrm{i}\beta_i\right). \tag{24}$$

Table 1 Convergence of the complex velocity at $z = (1.5, 0)$ in Fig. 1 for various modes, s

s	Direct solution	Indirect solution
0	(0.13894587,−0.12880990)	(0.10165966,−0.18257956)
1	$(1.23144822 \times 10^{-2}, -0.18278211)$	$(2.83025569 \times 10^{-2}, -0.23917957)$
2	$(9.87628883 \times 10^{-3}, -0.24458405)$	$(2.58406346 \times 10^{-2}, -0.24024898)$
3	$(2.82691706 \times 10^{-2}, -0.24682966)$	$(2.57877286 \times 10^{-2}, -0.24027159)$
4	$(2.84088388 \times 10^{-2}, -0.23889997)$	$(2.57866022 \times 10^{-2}, -0.24027208)$
5	$(2.52694375 \times 10^{-2}, -0.23902426)$	$(2.57865782 \times 10^{-2}, -0.24027209)$
10	$(2.57727429 \times 10^{-2}, -0.24027770)$	$(2.57865777 \times 10^{-2}, -0.24027209)$
15	$(2.57866454 \times 10^{-2}, -0.24027225)$	$(2.57865777 \times 10^{-2}, -0.24027209)$
20	$(2.57865796 \times 10^{-2}, -0.24027208)$	$(2.57865777 \times 10^{-2}, -0.24027209)$
50	$(2.57865777 \times 10^{-2}, -0.24027209)$	$(2.57865777 \times 10^{-2}, -0.24027209)$

Table 2 Comparison of the exact velocity magnitude with that obtained by the point-island approximation at various points, z, in the z-plane

z	PIA	ER	Error
(1.5,0)	0.1575	0.2416	34.8
(1.5,1)	0.2410	0.2060	17.0
(1.5,1.5)	0.2778	0.2169	28.1
(1.5,2)	0.2653	0.2133	24.4
(1.5,3)	0.1874	0.1681	11.5
(1.5,4)	0.1309	0.1261	3.8
(1.5,5)	0.0987	0.0986	0.2
(1.5,10)	0.0968	0.0808	3.0
(1.5,20)	0.0214	0.0219	3.0
(1.5,100)	0.00042	0.00042	0.5

Equation 24 expresses that, when the cylinders and the point vortex are far away with respect to the largest radius, then the total velocity is represented as a velocity due to a point vortex plus a velocity generated by dipoles placed at the centre of each cylinder (the point-island approximation). This approximation was first suggested by Johnson and McDonald [13] in which the effect of the approximation on the dynamics of two-dimensional vortices was examined. The image vortex pair of equal but opposite strength we employ, is mathematically equivalent to a dipole distribution of constant strength (equaling the vortex strength) on the line connecting the two vortices with a direction perpendicular to that line. On a field point far away the image vortex pairs can thus be approximated by single dipoles. The images and images of images can then even be summed and might be approximated by a single dipole, the strength and direction of which can be calculated with the boundary conditions.

The mathematical justification of the approximation is given in this paper. The region of validity of this approximation is established here by extensive numerical results. From (24) and (7) we see that, as the observation point moves away from the cylinders, "the point-island approximation" should give good results. This is verified in Table 2. The last column in Table 2 is the relative error in percentages and PIA stands for the point-island approximation and ER for the exact result.

We can also observe that, as ε_R gets smaller relative to ε_v, that is, as the cylinders move far away from each other but the point vortex is still close to one of the cylinders, the dipole approximation should give good results. In order to verify this numerically, we consider a second geometry in which there is a cylinder at the origin with unit radius but the second cylinder is at the position (0, 6), again with unit radius (Configuration 2). Our prediction is

Table 3 Relative percentage errors for the magnitude of the velocity obtained by the point-island approximation in Configurations 1 and 2; z is the observation point

z	Configuration 1	Configuration 2
(1.5,0)	34.8	27.5
(1.5,1)	17.0	1.4
(1.5,1.5)	28.1	7.0
(1.5,2)	24.4	7.4
(1.5,3)	11.5	7.1
(1.5,10)	3.0	0.9

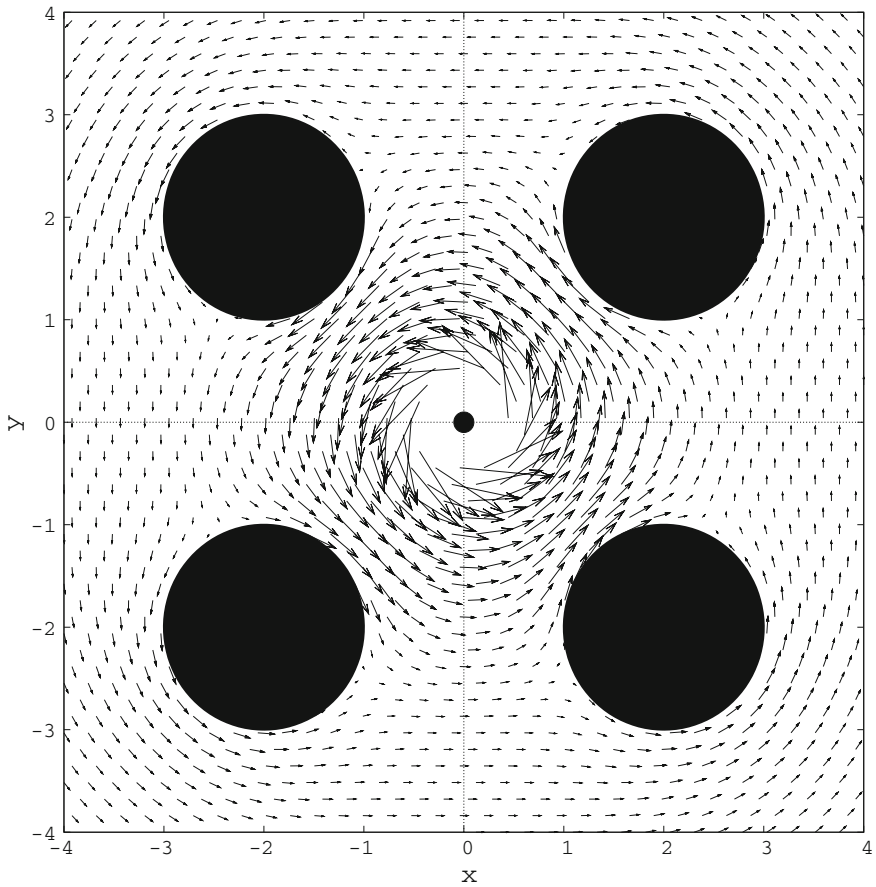

Fig. 2 Velocity distribution around four cylinders with a vortex at (0, 0) with strength -0.418

that the point-island approximation should give better results with Configuration 2 than with Configuration 1. This is confirmed by Table 3.

Next, we consider an example of four disks placed at the corners of a square, which resembles the legs of a Tension Leg Platform (TLP). This application can also be used to model flow around marine risers (see Fig. 2).

4.3 Vortex motion around N cylinders

Up to now, we have considered the velocity distribution at a fixed moment of time. Now we shall observe the motion of a vortex in the time domain in which the vortex is allowed to move with the flow. Its motion is governed by

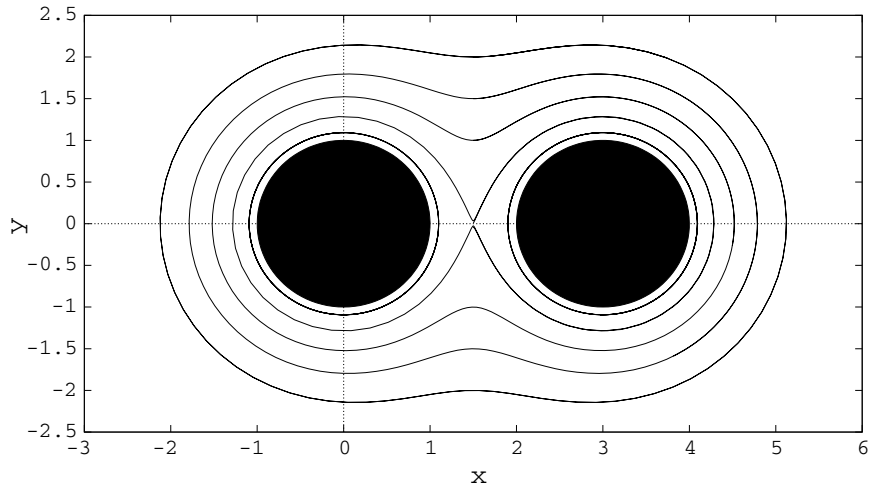

Fig. 3 Trajectory of motion of a single vortex around two cylinders

$$\dot{z}_0 = -\mathrm{i}\kappa \sum_{j=1}^{N}\sum_{n=1}^{\infty} A_n^j \frac{\left(\zeta_{0j}'\right)^n}{\zeta_{0j}^{n+1}} = -\mathrm{i}\kappa \sum_{j=1}^{N}\sum_{n=1}^{\infty} A_n^j \left(\frac{a_j}{|\zeta_{0j}|}\right)^{2n} \frac{1}{\zeta_{0j}}. \tag{25}$$

If the cylinders and vortex are far away from each other, we have

$$\dot{z}_0 = -\mathrm{i}\kappa\varepsilon_v \sum_{i=1}^{N} \frac{a_i}{(z_0 - z_i)^2} \exp\left(-\mathrm{i}\beta_i\right) \tag{26}$$

by the point-island approximation (24). In order to solve the above nonlinear differential equations, the standard Runge–Kutta method is used, and this was good enough for the configurations considered in this paper. However, for more complicated geometries, adaptive stepsize control for Runge–Kutta may be necessary. The trajectory of motion of a vortex around two cylinders is shown in Fig. 3, which is also given by Johnson and McDonald for cylinders of differing radii. The trajectory of motion of a vortex around four cylinders placed at the vertices of a square is interesting (see Fig. 4). We notice that the centre of the geometry is a stable centre point, whereas for two cylinders, the midpoint of the cylinders is a saddle point (unstable). In both configurations, if the vortex is close enough to one of the cylinders, it will rotate around that cylinder. In other words, the centre of any cylinder is a centre point.

5 Conclusions

An analytical–numerical method has been developed, using complex analysis, to solve the hydrodynamic interaction between an arbitrary number of cylinders and vortices. In this method the infinite power series within its domain of convergence represents an analytic function of a complex variable. The evaluation of the analytic function at specific points in the domain was carried out by taking a sufficient number of terms from the series to achieve a desired accuracy. In this approach there is no approximation of the boundary or the data; the solution exactly satisfies the boundary conditions at the exact boundary. The convergence of series (13) is not difficult to establish since the rate test gives convergence in the region $|\zeta_j| < |R_{ij}|$ or $|z - z_j| < |z_i - z_j|$. However, the full system (14) includes a double series, and it is not easy to establish a region of convergence in this case. This is why the convergence properties of the solution have not been studied analytically but numerically. The convergence properties of the infinite system used for determining the unknown coefficients is studied and found to be quite good. The domain of convergence for the point-island approximation is also studied.

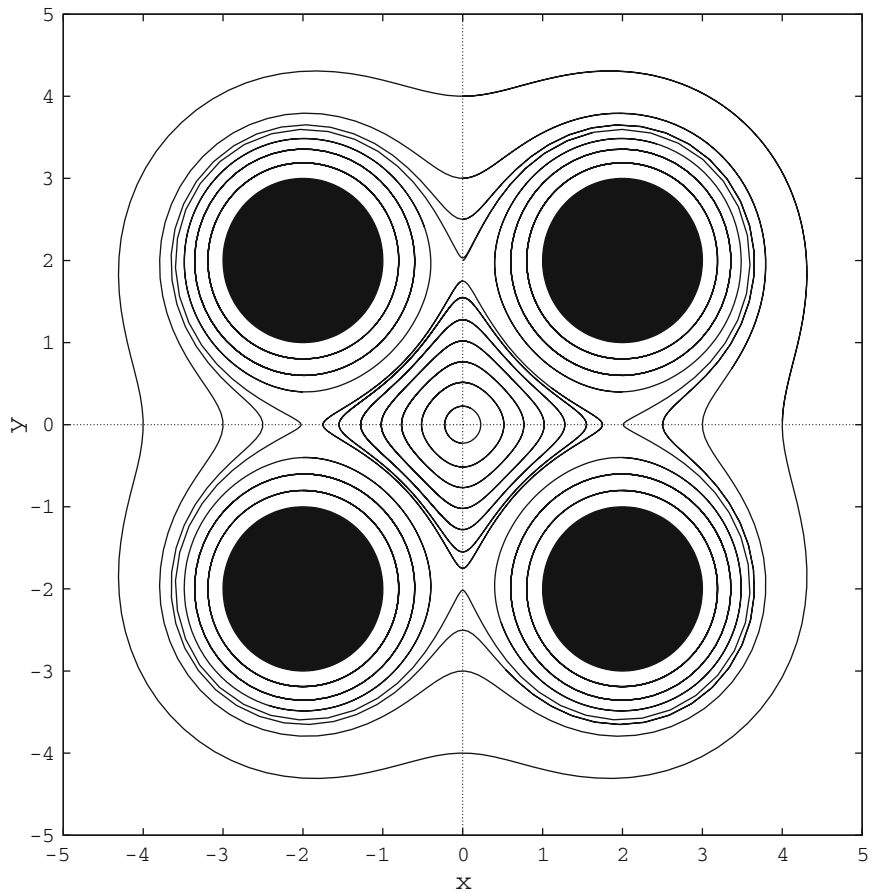

Fig. 4 Trajectory of motion of a single vortex around four cylinders

Extension of the results of this paper to an arbitrary number of vortices is trivial if the vortices are fixed in the plane (that is, the problem is solved for fixed moments of time). However, the motion of an arbitrary number of vortices with an arbitrary number of fixed cylinders is not integrable and this is not the subject of this paper. As is well known, in unbounded flow with more than $N_* = 3$ vortices the problem is not integrable; moreover, the introduction of boundaries into the fluid domain in general will reduce N_* [19].

Acknowledgements This study was carried out with support from TUBITAK (The Scientific and Technological Research Council of Turkey), Grant No 106T447 and Izmir Institute of Technology. The authors are also grateful to the referees, who suggested several important improvements to the presentation of the results.

References

1. Spring BH, Monkmeyer PL (1974) Interaction of plane waves with vertical cylinders. In: Proceedings of the 14th international conference on coastal engineering, vol 107, pp 1828–1845
2. Kagemoto H, Yue DKP (1986) Interactions among multiple three dimensional bodies in water waves: an exact algebraic method. J Fluid Mech 166:189–209
3. Linton CM, Evans DV (1990) The interaction of waves with arrays of vertical circular cylinder. J Fluid Mech 215:549–569
4. Yilmaz O (1998) Hydrodynamic interactions of waves with group of truncated vertical cylinders. J Waterw Port Coast Ocean Eng 124:272–279
5. Martin PA (2006) Multiple scattering: interaction of time-harmonic waves with *N* obstacles. Cambridge University Press, Cambridge

6. Johnson ER, McDonald NR (2004) The motion of a vortex near two circular cylinders. Proc R Soc Lond A 460:939–954
7. Burton DA, Gratus J, Tucker RW (2004) Hydrodynamic forces on two moving discs. Theor Appl Mech 31:153–188
8. Crowdy D, Marshall J (2005) Analytical formulae for the Kirchhoff–Routh path function in multiply connected domains. Proc R Soc Lond A 461:2477–2501
9. Pashaev O, Yilmaz O (2008) Vortex images and q-elementary functions. J Phys A Math Theor 41:135207
10. Crowdy D, Marshall J (2005) The motion of a point vortex around multiple circular cylinders. Phys Fluids 17:056602
11. Crowdy D, Marshall J (2006) The motion of a point vortex through gaps in walls. J Fluid Mech 551:31–48
12. Katz J, Plotkin A (2001) Low-speed aerodynamics. Cambridge University Press, Cambridge
13. Johnson ER, McDonald NR (2005) The point island approximation in vortex dynamics. Geophys Astrophys Fluid Dyn 99(1):49–60
14. Fin MD, Cox SM, Byrne HM (2003) Topological chaos in inviscid and viscous mixers. J Fluid Mech 493:345–361
15. Price TJ, Mullin T, Kobine JJ (2003) Numerical and experimental characterization of a family of two-roll-mill flows. Proc R Soc Lond A Math Phys Eng Sci 459:117–135
16. Hellou M, Coutanceau M (1992) Cellular stokes flow induced by rotation of a cylinder in a closed channel. J Fluid Mech 236:557–577
17. Milne-Thomson LM (1968) Theoretical hydrodynamics. Macmillan, London
18. Antoine X, Chniti C, Ramdani K (2008) On the numerical approximation of high frequency acoustic multiple scattering problems by circular cylinders. J Comput Phys 227:1754–1771
19. Aref H (1983) Integrable, chaotic, and turbulent vortex motion in two dimensional flows. Annu Rev 15:345–389